JGR Oceans

RESEARCH ARTICLE
10.1029/2019JC015050

Key Points:
- An Eulerian, three-dimensional marine microplastic distribution model
- A microplastic plastic distribution model including negatively buoyant plastics
- Microplastic debris is present throughout water column and on sea floor

Correspondence to:
A. S. Mountford,
a.s.mountford@newcastle.ac.uk

Citation:
Mountford, A. S., & Morales Maqueda, M. A. (2019). Eulerian Modeling of the Three-Dimensional Distribution of Seven Popular Microplastic Types in the Global Ocean. *Journal of Geophysical Research: Oceans*, *124*. https://doi.org/10.1029/2019JC015050

Received 19 FEB 2019
Accepted 28 OCT 2019
Accepted article online 16 NOV 2019

Eulerian Modeling of the Three-Dimensional Distribution of Seven Popular Microplastic Types in the Global Ocean

A. S. Mountford[1] and **M. A. Morales Maqueda**[1]

[1]School of Natural and Environmental Sciences, Newcastle University, Newcastle upon Tyne, UK

Abstract Detailing the distribution of past and future plastic debris in the marine environment has become a pressing challenge. Plastic pollution poses a potential threat to marine organisms and the marine environment as a whole. Previous studies using Lagrangian particle models have identified five garbage patches within subtropical ocean gyres, with the possibility of a sixth garbage patch within the Barents Sea. We present the first coarse resolution three-dimensional plastic distribution model to use an Eulerian approach. It considers seven plastic components, three of them buoyant and four nonbuoyant, based upon real world plastic types. Our control results support the observations of positively buoyant plastic accumulations within the five garbage patches. However, there is no evidence of a sixth garbage patch in the Barents Sea. Meanwhile, our simulations reveal a previously unreported accumulation of plastic in the Gulf of Guinea. The negatively buoyant plastic tends to accumulate within the deepest regions of the sea floor, loosely following the bathymetry. In two further experiments, we introduce idealized plastic removal rates to simulate the proportion of plastics that are sequestered within sediments once they reach the sea floor. The results of the simulations show that substantial quantities of plastic debris are subject to vertical transport in the ocean and are therefore present throughout the water column as well as on the sea floor. A final experiment, focusing on neutrally buoyant plastics, shows the potentially ubiquitous presence of small microplastics and nanoplastics in the water column.

Plain Language Summary Detailing the distribution of past and future plastic debris in the ocean has become a pressing challenge. Plastic pollution poses a potential threat to marine organisms and the marine environment as a whole. The use of numerical modeling has identified five garbage patches, with the possibility of a sixth garbage patch in the Arctic. However, these models have focused on plastics that float on or near the sea surface and do not consider the plastics which sink or are drawn down once they enter the ocean. We present the first plastic distribution model, which includes both floating and sinking plastics and looks at the distribution of these plastics throughout the water column. Both types of plastics are present throughout the water column, with the floating plastics mainly collecting within the five previously identified garbage patches and the sinking plastics gathering within the deepest areas of the seafloor. Simulations including a crude mechanism by which plastics are removed into the seafloor "sediments," reveal wide-spread areas of the seafloor, which may host large amounts of plastic debris. An experiment with neutrally buoyant plastic tracers that mimics the behavior of microplastics and nanoplastics shows these plastics to be present at all depths globally.

1. Introduction

Global plastic production in 2016 reached 335 million metric tons, bringing the estimated total of virgin plastics ever produced to almost 8.7 billion metric tons (Geyer et al., 2017; PlasticsEurope, 2017). In recent years, the global consumption of single-use plastics, such as carrier bags, plastic straws, and drinks bottles, has been of particular concern as we find ourselves immersed in a "throwaway" culture, with single-use plastics making up around 80% of plastics entering the marine environment (McDermott, 2016). Most recent estimates suggest that around 15 million metric tons of plastics enter the world's oceans per year, with between 4.8 and 12.7 million metric tons coming from coastal land sources and up to 2.4 million metric tons coming from inland and river inputs (Jambeck et al., 2015; Lebreton et al., 2017). Land sources are expected to account for between 75% and 90% of marine litter, with the remaining 10–25% coming from ocean sources, such as fishing (Li, 2018). Marine plastic pollution was first documented in the 1970s and

has since become a popular topic, not only within the scientific community but with the media and general population (Law, 2017). Once plastic enters seas and oceans it can have a detrimental effect on the marine environment itself, such as through gas exchange inhibition in sediments (Derraik, 2002), as well as on a wide range of marine organisms, through entanglement and ingestion (and associated toxicity implications) (Gregory, 2009).

Despite the large estimated rate of plastic entering the marine environment, current estimates from sampling and modeling studies have accounted for only between 98 and 236 thousand metric tons of floating plastic debris in the world's oceans (Eriksen et al., 2014; van Sebille et al., 2015). These estimates leave well over 99% of all plastics ever to have entered the oceans unaccounted for. A number of possible sinks have been proposed, such as deep-sea sediments, resuspension within the water column, shore deposition, and ingestion by marine organisms (Cózar et al., 2014), but quantification of the amounts of plastics in each of these areas has not yet been achieved. Sampling efforts have shown a ubiquitous presence of plastic debris within the marine environment, from shorelines to the seafloor, including the water column, deep-sea sediments and sea ice (Law, 2017). As such, modeling estimates that only take into account floating plastic particles at the sea surface are expected to be highly conservative and ignore potentially substantial sinks for the global ocean plastic budget by not taking into account the full water column. There is currently a need for a better understanding of the possible removal processes of plastics from the sea surface, for instance, the fragmentation rates of plastics of all types and the associated effect of fragmentation on rising and sinking rates (Hardesty et al., 2017), and density changes caused by biofouling (Kooi et al., 2017).

Both modeling and observational efforts have confirmed the existence of five accumulation zones in the surface layers of the ocean, within subtropical ocean gyres. These five accumulations, or “garbage patches,” have been shown to exist in the North and South Pacific, North and South Atlantic, and Indian Oceans. Recent model simulations suggest the potential of a sixth accumulation zone within the Barents Sea, in the Arctic Ocean (van Sebille et al., 2012). These modeling efforts focus only on buoyant plastic floating at or near the surface. The purpose of the research presented in this article is to do a preliminary exploration with a general circulation ocean model of how positively and negatively buoyant plastic components become dispersed through the water column and the sea floor under the combined effects of ocean currents and turbulence. This paper will give a description of the model (section 2), followed by details of the outputs of the model (section 3). The results are divided into positively and negatively buoyant plastic types for the control experiment and the first two of the sensitivity experiments, followed by the results of the outputs from the neutrally buoyant plastic sensitivity simulation. Conclusions and a summary of the findings and their place within the literature will conclude the paper (section 4).

2. Materials and Methods

2.1. Model Description

This study uses the state-of-the-art model Nucleus for European Modelling of the Ocean Version 3.6, configuration ORCA2-LIM3, an Eulerian, rather than Lagrangian, formulation to simulate the three-dimensional dispersion of plastics in the global ocean. There are advantages and disadvantages to both Eulerian and Lagrangian approaches, and the two approaches most likely complement one another. A Lagrangian formulation focuses on an individual particle's trajectory, whereas an Eulerian framework describes particles in terms of their mass or volume concentrations—and possibly other particle properties—which are advected by the ocean's velocity field and diffused by parameterized and resolved turbulence, which, in Lagrangian models needs to be represented as ad hoc random motions (van Sebille et al., 2018). As we are dealing with large concentrations of plastic waste, and we are more concerned with global patterns of distribution than the behavior of individual plastic particles, an Eulerian approach was a more appropriate choice for the present study. It also lends itself more readily to the representation of the three-dimensional distribution created by the combined effects of mean flow and eddy transports. The ORCA2-LIM3 configuration is of relatively coarse resolution, based on a global 2° Mercator horizontal mesh with a 1° meridional refinement in tropical and equatorial regions and a bipolar cap north of about 30°N. There are 31 vertical levels, 10 of which are located in the upper 100 m. The resolution in the deepest parts of the ocean is 500 m but the bottom boundary layer scheme of Beckmann and Döscher (1997) is used to represent transport near the sea floor. The depth of the bottom cell is adjustable to better represent

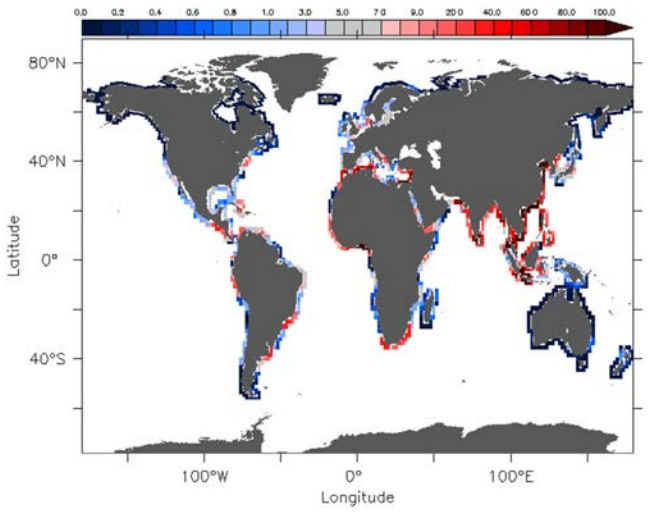

Figure 1. Annual plastic input relative to the average plastic input per unit area. Data supplied by van Sebille et al. (2015), based upon global mismanaged waste data from 2010 as described in Jambeck et al. (2015).

bathymetry gradients (Pacanowski & Gnanadesikan, 1998). The time step is 5,760 s. The horizontal viscosity is 40,000 $m^2\ s^{-1}$, except within 20° north and south of the equator where, away from western boundary currents, it decays linearly to 2,000 $m^2\ s^{-1}$. Lateral eddy transport includes along-isopycnal diffusion, with a diffusivity of 2,000 $m^2\ s^{-1}$, and eddy-induced advection à la Gent and McWilliams (1990). Vertical mixing through the water column is parameterised using the order 1.5 turbulent closure scheme of Blanke and Delecluse (1993). Vertical viscosities and diffusivities are ramped up to 10 $m^2\ s^{-1}$ in case of hydrostatic instability. The equation of state is the recommended by the TEOS-10 team (IOC, SCOR, and IAPSO, 2010). For a more detailed description of the ORCA2-LIM3 configuration see, for example, Madec (2015) and Vancoppenolle et al. (2008), Belamari and Pirani (2007), and Timmermann et al. (2005).

Plastic tracers were added through the creation of a "Plasticene" configuration, using plastic waste input data from van Sebille et al. (2015), modified from estimated plastic waste inputs to the ocean for the year 2010 from Jambeck et al. (2015). The plastic inputs are distributed along the coastlines in proportion to the total population within 200 km of the sea (Figure 1). Only around Antarctica and in the high Arctic (above approximately 70°N) sources are 0. Due to its coarse resolution, the coastlines in the model only approximately follow the real ocean-land boundaries, resulting in the obvious discrepancies between the locations of plastic sources in the model and the continental outlines depicted.

For a given plastic type, the model's change in concentration (mass per volume) of plastic (C) over time (t) is governed by

$$\frac{\partial C}{\partial t} = -\vec{\nabla}_H(\vec{u}C) - \frac{\partial(wC)}{\partial z} + \vec{\nabla}_H\left(K_H\vec{\nabla}_H C\right) + \frac{\partial}{\partial z}\left(\varkappa\frac{\partial C}{\partial z}\right) - w_r\frac{\partial C}{\partial z}, \quad (1)$$

where $\vec{\nabla}_H$ is the horizontal gradient operator; $\vec{u}$ is the horizontal advection flux (which includes the Eulerian current plus a Gent-McWilliams transport term, Gent, 2011); w is, similarly, the combined Eulerian current plus Gent-McWilliams vertical velocity; z is the vertical coordinate; K_H is the horizontal component of the Redi diffusivity (Redi, 1982); $\varkappa$ is the vertical, Redi plus diapycnal, diffusivity; and w_r is the rise velocity of plastic, which, in this simple formulation, is calculated by postulating a balance between plastic buoyancy and friction (as described in equation (4)).

At the surface, we assume no advective or turbulent flux of plastic other than at the land boundaries. The advective bottom flux (F_b) is given by

$$F_b = w_s C_b, \quad (2)$$

where C_b is concentration of plastic in the bottom grid cell and w_s is a prescribed, negative piston velocity. In the control simulation, $ws = 0$, but will be different from zero in two plastic sedimentation sensitivity experiments, as described in sections 3.3.4 and 3.3.5. Turbulent fluxes and rise/sink velocities are set to zero at the bottom.

All experiments were started from a plastic-free state after a 10 year spin-up of the ocean hydrography. The surface atmospheric fluxes were calculated from the Corrected Normal Year CORE data (Large & Yeager, 2009) directly provided with the Nucleus for European Modelling of the Ocean code. Throughout the simulations, including the spin-up period, the ocean temperature, and salinities were restored to World Ocean Atlas annual mean observations (Locarnini et al., 2013; Zweng et al., 2013) with a relaxation e-folding timescale of 1 year. The speed and direction of the global, annual mean surface currents calculated by the model are shown in Figure 2. The model exhibits seasonal but virtually no interannual variability.

The coastal pattern of plastic release was maintained constant through the simulation, but the actual amount of plastic entering the ocean was gradually ramped up in order to reflect the projected

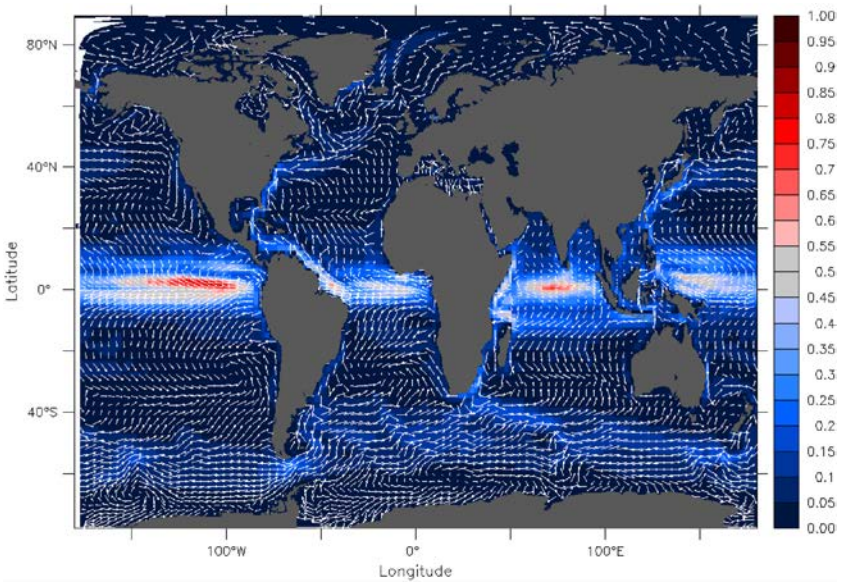

Figure 2. Global, annual mean surface currents (m s^{-1}). Speed is shown in color, while unit vectors indicate direction (every other vector is shown).

increasing plastic production and inputs in the future (Ryan, 2015; Wilcox et al., 2015). This ramp up factor (R) is

$$R = 2^{(y-50)/100}, \tag{3}$$

where y is the year number (van Sebille, personal communication). When y is 0, the total input of plastics is approximately 7.2 million metric tons per year, and when y is 50 this figure is closer to 10 million metric tons per year. These inputs are at the higher end of estimated inputs into the oceans. However, for our purposes, the patterns of distributions are more important than the plastic concentrations themselves; hence, all the results we present focus on the proportion of plastic relative to the average concentration.

Our plastic dispersion model considers the seven most common plastic types in production—high-density polyethylene (HDPE), low-density polyethylene, polyvinyl chloride (PVC), polystyrene (PS), polypropylene (PP), polyethylene terephthalate (PET), and polyurethane (PUR)—with rise and sink velocities based upon the respective plastic densities, as listed in Table 1 (Andrady & Neal, 2009; PlasticsEurope, 2017). Four out of these seven plastic types (PVC, PS, PET, and PUR) are negatively buoyant, with associated sink velocities. This reflects the prediction that 70% of plastic debris entering the marine environment will sink and remain on the sea floor (Frias et al., 2016). The rise and sink velocities (w_r) were calculated based on postulating a balance between buoyancy and friction according to

$$w_r = \frac{|\rho_w - \rho_p|}{\rho_w - \rho_p}\sqrt{\frac{|\rho_w - \rho_p| gL}{\rho_p}}, \tag{4}$$

where ρ_p is the density of the plastic type, L is a frictional length scale, here given a constant and uniform value of approximately 10^{-6} m, ρ_w is the seawater density calculated by the model, and g is gravitational acceleration. Note that since ρ_w is a three-dimensional field, so is w_r. The use of a linear Stokes' friction law, rather than the quadratic formulation adopted in (4), might have been more appropriate since the rise velocities, and therefore, their associated Reynolds numbers, are small. However, rise velocities are expected to vary considerably, even for a given plastic type, as a function of plastic geometry, age, biological load, and other factors. Although there is no explicit plastic particle size in this model, since

Table 1
Seven Most Common Plastic Types (as Listed in PlasticsEurope (2017)) With Their Associated Densities and Rise Velocities (Calculated for ρ_w = 1,025 kg/m^3) (Andrady & Neal, 2009)

Plastic type	Density (kg/m^3)	Average density (kg/m^3)	Rise velocity (m/s)
HDPE	940–970	955	0.00085
LDPE	920–940	930	0.001
PVC	1,150–1,350	1,250	−0.0013
PS	1,040	1,040	−0.00038
PP	970–1,050	1,010	0.00038
PET	1,300–1,400	1,350	−0.00154
PUR	871–1,420	1,145.5	−0.00102

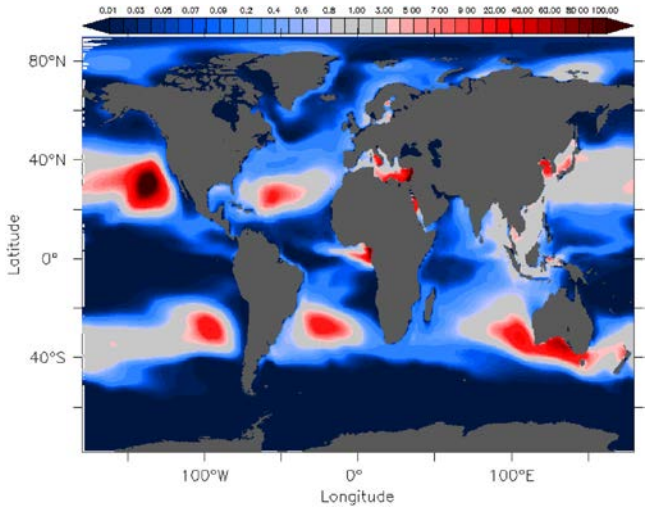

Figure 3. Accumulation of positively buoyant plastics (HDPE, LDPE, and PP) after a 50 year simulation in the control experiment. Shown is the plastic concentration relative to the global average concentration of plastics.

we use plastic mass concentrations, the chosen frictional length scale implies that the effective particle size is ~0.1 mm for $|\rho_w - \rho_p| = 10$ kg m^{-3} and ~0.06 mm for $|\rho_w - \rho_p| = 100$ kg m^{-3}. Although w_r is a three-dimensional field, our choice of L and $\rho_p$lead to typical absolute values for the rise velocity of about 1 mm s^{-1}, which are commensurate with observations (Reisser et al., 2015).

2.2. Experimental Design

Four experiments were conducted as follows. In the control simulation, once any plastic components reach the sea floor (the bottommost grid cell of the model) they are subject to transport by bottom currents with no removal processes. In reality, it would be expected that a potentially large proportion of the plastic particles that reach the sea floor would be incorporated and sequestered within the sediment (Van Cauwenberghe et al., 2015). To investigate the impact on plastic distribution of a simple mechanism of plastic removal into the sediments, two sensitivity simulations were carried out in which a plastic sedimentation rate was prescribed according to equation (2) with a uniform, nonzero sedimentation velocity. Finally, a third sensitivity experiment was conducted, in which all plastic was assumed to be neutrally buoyant and $w_s = 0$.

In the first of these three sensitivity simulations, the piston velocity was set at the value of 90 m year^{-1}. In the second experiment, a smaller value was chosen for w_s, with a value of 30 m year^{-1}. Literature on the dynamics and timescales of plastic incorporation into both marine and freshwater sediments are limited (such as Corcoran et al., 2015; Gilligan et al., 1992; Turner et al., 2019; Wessel et al., 2019), particularly with regard to values which could be used as a global average, and so, our approach to modeling this process is very tentative. Using a piston velocity formulation to simulate plastic sedimentation leads to *e*-folding timescales for plastic removal that depend on the depth of the water column. For example, in a water column with a depth of 90 m the first piston velocity would lead to an *e*-folding timescale of 1 year, while the second would be associated with an *e*-folding timescale of three years. These timescales are significantly shorter than the length of our simulations. While this model has no parameterization for the beaching of plastics, this near-coast flux of both positively and negatively buoyant plastics into the sediments could be thought of as a coarse approximation of beaching.

The third sensitivity simulation focuses on neutrally buoyant plastics. The reason for considering neutrally buoyant plastics in this study is as follows. The upward buoyant force on a piece of plastic of arbitrary shape is proportional to the volume of the object. In contrast, the friction that counters the buoyant force as the plastic piece moves through the water is proportional to the cross-sectional area of the former (e.g., Batchelor, 1967) and, for creeping flows (at relatively small velocities), to the radius of a sphere with the same volume (Leith, 1987). As a result, the rise velocity of the object will normally tend to 0 as its volume tends to 0. For a spherical plastic particle with a size of 1 mm (the upper boundary for microplastics (Hartmann et al., 2019)) and a density of 955 kg m^{-3} (the average density of HDPE, a positively buoyant plastic type), its rise velocity would be approximately 0.035 m s^{-1}. However, for a particle of the same material but 1 μm in size (the boundary between microplastics and nanoplastics (Hartmann et al., 2019)) the rise velocity would be one hundred thousand times smaller. Based on this line of argument, Kooi et al. (2017) hypothesize that there may be eventually be a uniform distribution of nanoplastic particles within the water column, since they will behave as passive tracers as their rise velocity is negligible.

3. Results and Discussion

3.1. Positively Buoyant Plastics

3.1.1. Control Experiment

At the end of a 50 year simulation, the positively buoyant plastic components (HDPE, low-density polyethylene, and PP) show accumulation within the five documented "garbage patches" (Lebreton et al., 2012; Maximenko et al., 2012; van Sebille et al., 2012; van Sebille et al., 2015), as seen in Figure 3, with accumulations shown to be above the global average concentration. The North Pacific is the area of greatest

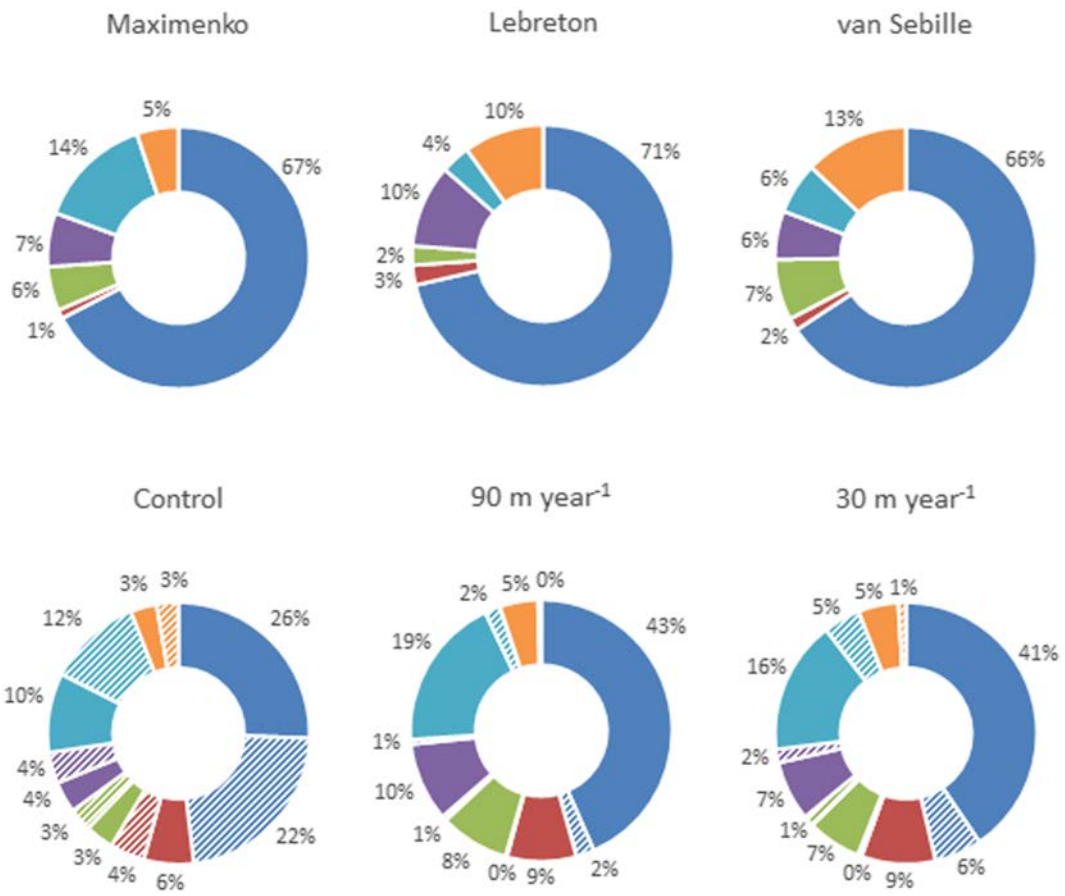

Figure 4. Proportion of positively (HDPE, LDPE, and PP—solid color) and negatively (PVC, PS, PET, and PUR—striped) buoyant plastics in each of the major basins in **(a)** Maximenko et al. (2012), **(b)** Lebreton et al. (2012), **(c)** van Sebille et al. (2015), **(d)** the control experiment, **(e)** the 90 m year^{-1} sedimentation rate experiment, and **(f)** the 30 m year^{-1} sedimentation experiment. Blue = North Pacific, red = South Pacific, green = North Atlantic, purple = South Atlantic, turquoise = Indian, and orange = Mediterranean.

accumulation, accounting for approximately half of the total positively buoyant plastics released in the control simulation (Figure 4d). The outcome that the North Pacific retains the greatest quantities of floating plastic debris is in accordance with previous modeling research (Figures 4a–4c). However, the results from the present study suggest that the accumulations in the North Pacific may be overestimated in relation to the other accumulations in other modeling studies. It must be noted that the present simulations are run on a shorter timescale than the simulations of Lebreton et al. (2012), Maximenko et al. (2012), and van Sebille et al. (2015). However, the 50 year timescale used in the present study was decided upon for comparisons to real-life plastic timescales. The divisions into the major ocean basins used in this research are shown in Figure 5. Aside from the accumulations in the "garbage patches," there are also visibly high concentrations in the Mediterranean, off the west coast of Africa within the Gulf of Guinea, within Southeast Asia, and off the south coast of Australia. This accumulation off the south coast of Australia is a combination of drift from the Indian Ocean "garbage patch," transported by the Leeuwin Current (Thompson, 1984) and inputs in the region becoming trapped in the Great Australian Bight.

The positively buoyant plastics are concentrated within the top 100–150 m of the sea surface within all ocean basins (Figures 6a–6h), except for in those that are present in the Mediterranean Sea (Figure 6h) and the Arctic Ocean (Figure 6f), which only reach depths of around 60–80 m. The Arctic Ocean has a particularly shallow distribution of positively buoyant plastics due to its highly stratified nature, with a cold, fresh surface layer formed by melt water (Björk, 1989). The buoyant plastics in the Southern Ocean, on the other hand, are drawn down to a greater depth of approximately 150 m (Figure 6g). Strong surface mixing results in greater

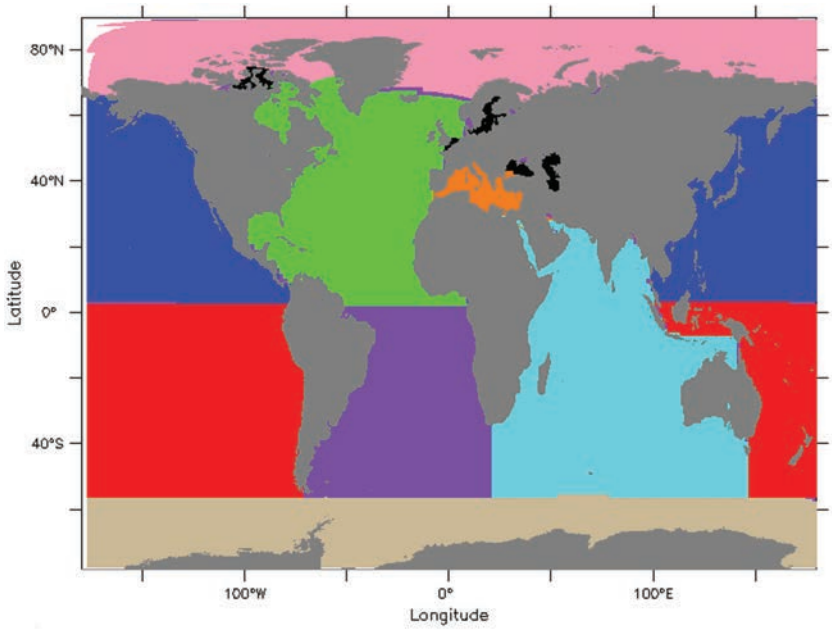

Figure 5. Geographic division of the basins used in this study. Blue = North Pacific, red = South Pacific, green = North Atlantic, purple = South Atlantic, cyan = Indian Ocean, orange = Mediterranean, pink = Arctic, and tan = Southern Ocean.

mixed layer depths (Dong et al., 2007). In the steady state and assuming that vertical advection and mixing are the key controls of the vertical plastic distribution, we would expect the concentration profiles to be described by $C_0 e^{\frac{w_r}{\kappa} z}$, where C_0 is the concentration at the surface. The simulated profiles are indeed approximately exponential in all the basins. Excluding the Mediterranean and both polar oceans, these profiles are also very similar and reach all down to about 100 m, indicating that the average levels of turbulent mixing in the upper ocean are also similar.

In this control simulation there is no presence of the proposed sixth garbage patch within the Barents Sea, as reported in van Sebille et al. (2012). However, an accumulation appears instead in the East Siberian, Chukchi, and Beaufort Seas (Figure 3). Inflows of plastic laden waters through the Bering Strait slowly converge toward the New Siberian Islands region and the Beaufort Sea gyre. How realistic these accumulations

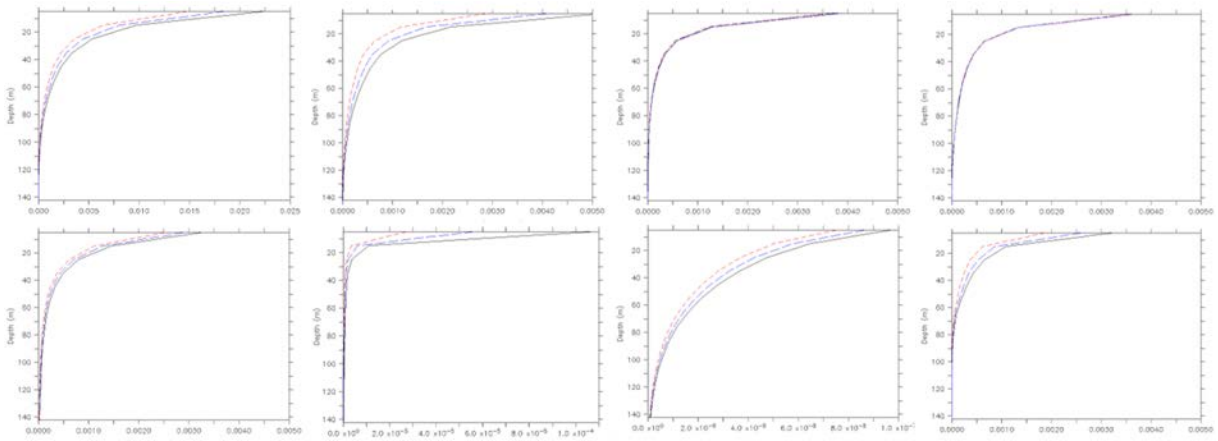

Figure 6. Vertical profile of positively buoyant plastics (HDPE, LDPE, and PP) (black line = control simulation, red dashed line = 90 m year^{-1} simulation, and blue dashed line = 30 m year^{-1} simulation)—(a) North Pacific, (b) South Pacific, (c) North Atlantic, (d) South Atlantic, (e) Indian, (f) Arctic, (g) Southern Oceans, and (h) Mediterranean Sea. (NB = differing scales). Shown is the basin averaged volumetric plastic concentration normalized by the global average.

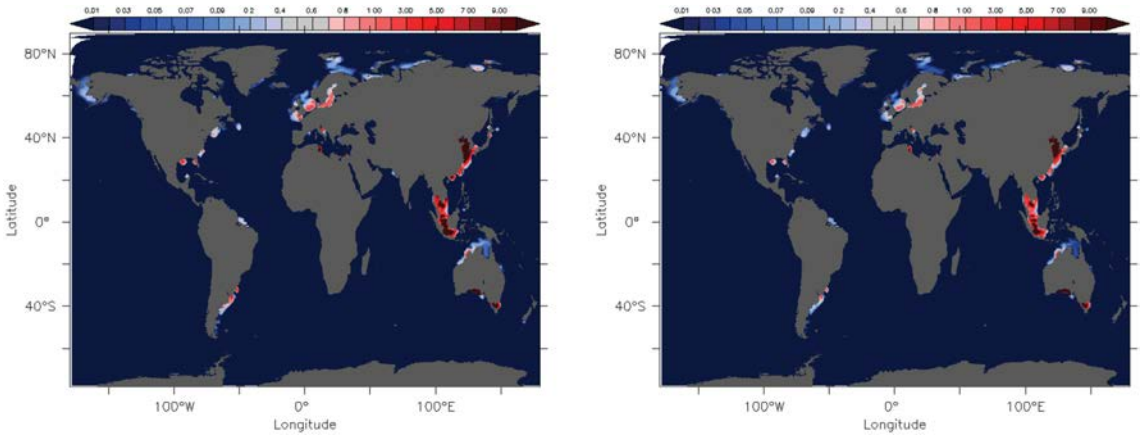

Figure 7. Flux of positively buoyant plastics (HDPE, LDPE, and PP) into the "sediments" at the end of a 50 year simulation, relative to the average global flux of plastics into the "sediments" per unit area with **(a)** 90 m year^{-1} piston velocity and **(b)** 30 m year^{-1} piston velocity.

are is difficult to judge, since our model ignores the role of sea ice in controlling the transport and accumulation of plastic in polar oceans. Sea ice plays an important role by trapping and releasing plastics, in particular buoyant microplastics (Lusher et al., 2015; Obbard et al., 2014). This is supported by Peeken et al. (2018), with reported concentrations of up to $(1.2 \pm 1.4) \times 10^7$ microplastic particles per m^3 of sea ice in the Fram Strait, suggesting that Arctic sea ice is a substantial temporal sink for microplastics. Van Sebille et al. (2012), who first reported the potential presence of an accumulation zone within the Barents Sea, draw a relation between this apparent accumulation and seasonal sea ice: The currents within the van Sebille et al. (2012) model were based upon surface buoy data, many of which may have become trapped in seasonal sea ice during winter.

High levels of plastic accumulation can also be seen in the Gulf of Guinea off the west coast of Africa (Figure 3), which have not been previously reported. Inputs from the area around Nigeria are the highest in the Atlantic (Figure 1), and as with the accumulations in the Arctic, surface water currents (Figure 2) are able to explain the patterns of accumulation that can be seen. The Guinea Current in combination with the Angola Current traveling northward form a large anticyclonic gyre in the Gulf of Guinea, in which the positively buoyant plastic components become trapped and accumulate (Gyory et al., 2005). Despite the outputs of this simulation suggesting high accumulations in this area, there are very few empirical data to support this. As such, the results of this simulation suggest that the Gulf of Guinea region may be a possible area of interest for future plastic sampling efforts.

3.1.2. Sensitivity Experiments

Qualitatively, the horizontal distribution of buoyant plastics in the sedimentation experiments does not greatly differ from that in the control run. Quantitatively, there is a reduction in the total global plastic load in the ocean of 30% and 16% in the 90 and 30 m year^{-1} piston velocity sensitivity experiments respectively. Regarding vertical distributions, the greatest relative decrease in positively buoyant plastics in these experiments can be seen in the South Pacific, Mediterranean, and Arctic (Figures 4d–4f and 6b, 6f, and 6h). The flux into the sediments is primarily in the vicinity of the coastlines, where the water is shallower and hence the positively buoyant plastics are close enough to the sea floor to be incorporated into the sediments (Figures 7a and 7b). The removal of plastics in Southeast Asia (North and South Pacific) is particularly visible. This coastal removal results in a reduction in the "drift" of plastics across the North and South Pacific (Figures 8a and 8b).

In both of the sedimentation simulations, the accumulation of plastics in the Arctic Ocean, particularly in the East Siberian, Chukchi and Beaufort seas, is not as pronounced as in the seven plastics control experiment after 50 years (Figures 8a and 8b). The differences between the control experiment and the two sensitivity experiments are explained by two factors. First, the plastic inflow through Bering Strait is reduced with respect to the control run (as part of the plastic entering the ocean is gradually deposited on the seafloor). Second, the plastic that accumulates in this Arctic region can also be removed from the water column by sedimentation. Indeed, the East Siberian Arctic Shelf (comprising of the East Siberian Sea and the Laptev

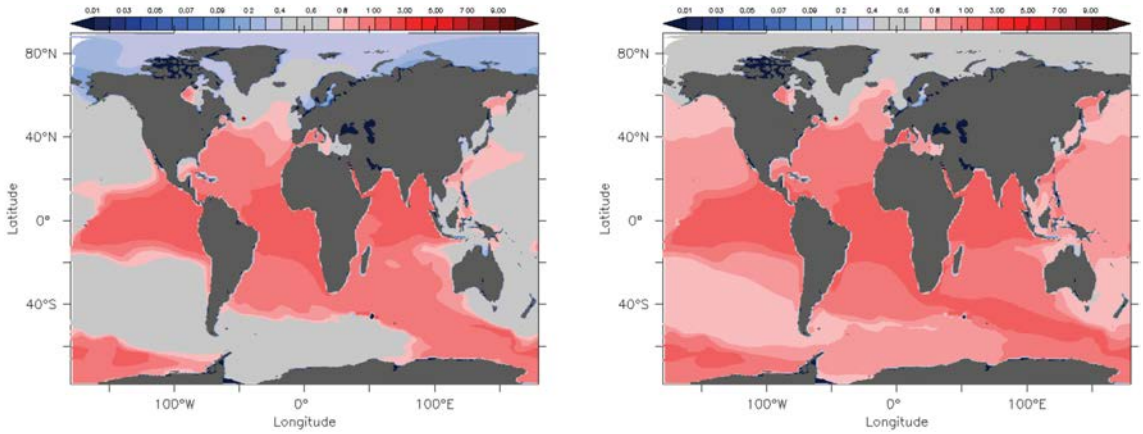

Figure 8. Difference between the concentration of positively buoyant plastics (HDPE, LDPE, and PP) in the control simulation and the sensitivity simulation with **(a)** 90 m year^{-1} piston velocity and **(b)** 30 m year^{-1} piston velocity after a 50 year simulation, relative to the global average concentration of plastics.

Sea) is very shallow, with a mean depth of 50 m (Alling et al., 2010). And so, the positively buoyant plastic components can be drawn down relatively easily by turbulence into the lowest grid cell and hence removed through sedimentation (Figures 7a and 7b).

3.2. Negatively Buoyant Plastics

3.2.1. Control Experiment

All current modeling research has focused on floating buoyant plastics and surface waters; hence, there are no modeled data against which to compare our nonbuoyant plastic simulations. While there are empirical data for a number of areas, including the deep sea (Chiba et al., 2018; Van Cauwenberghe et al., 2015) and polar regions (Barnes et al., 2009; Bergmann & Klages, 2012; Van Cauwenberghe et al., 2013), global plastic sediment data are lacking.

The highest accumulations of negatively buoyant plastics (PVC, PS, PET, and PUR) can be observed within the Mediterranean, off the west coast of Africa, and within Southeast Asia (Figure 9). The largest proportion of negatively buoyant plastics is within the North Pacific, although the Indian Ocean also has widespread accumulation (Figure 4). These accumulations appear to loosely follow the bathymetry, with the highest concentrations in the deepest areas, as can be seen in Figure 9. As there are no methods of removal for the plastic in this simulation, once the negatively buoyant plastics reach the sea floor they are subject to transportation by bottom currents, as well as the diffusive bottom boundary layer parameterisation of the model (Beckmann & Döscher, 1997). Because of this bottom boundary parameterisation, the plastic tracers can be seen "radiating" outward away from the coastline, as they continue to be transported until they reach the deepest areas of sea floor. This is particularly apparent in the Indian Ocean, with a complete lack of plastic accumulation along the Ninety East Ridge, which rises to between 1,500 and 2,000 m above the surrounding sea floor (Bowin, 1973).

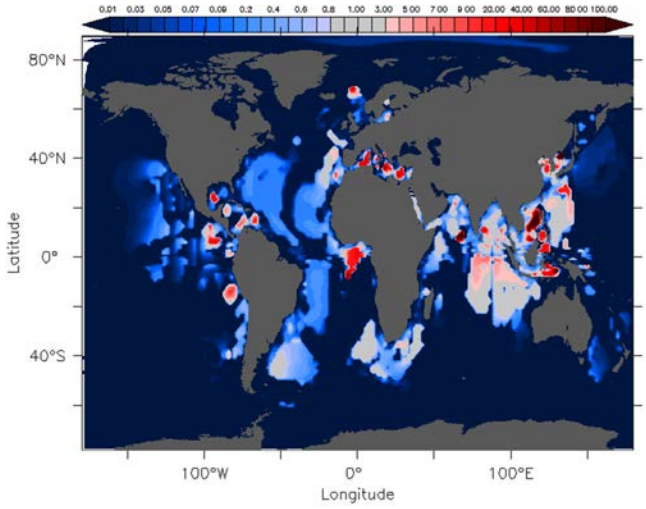

Figure 9. Accumulation of negatively buoyant plastics (PVC, PS, PET, and PUR) after a 50 year simulation in the control experiment. Shown is the plastic concentration relative the global average concentration of plastics.

3.2.2. Sensitivity Experiments

As expected, the introduction of a parameterisation of sedimentation has more of an impact on the negatively buoyant plastic components than on the positively buoyant components. There is a reduction in the total global plastic load in the ocean of 95% and 84% in the 90 and 30 m year^{-1} piston velocity sensitivity experiments. The North Pacific and Indian oceans are the basins most affected with the introduction of a piston velocity (Figures 4 and 10). Unsurprisingly, for the experiment with the higher sedimentation rate of 90 m year^{-1}, the plastic components do not spread as far away from the coastlines in comparison to the experiment with

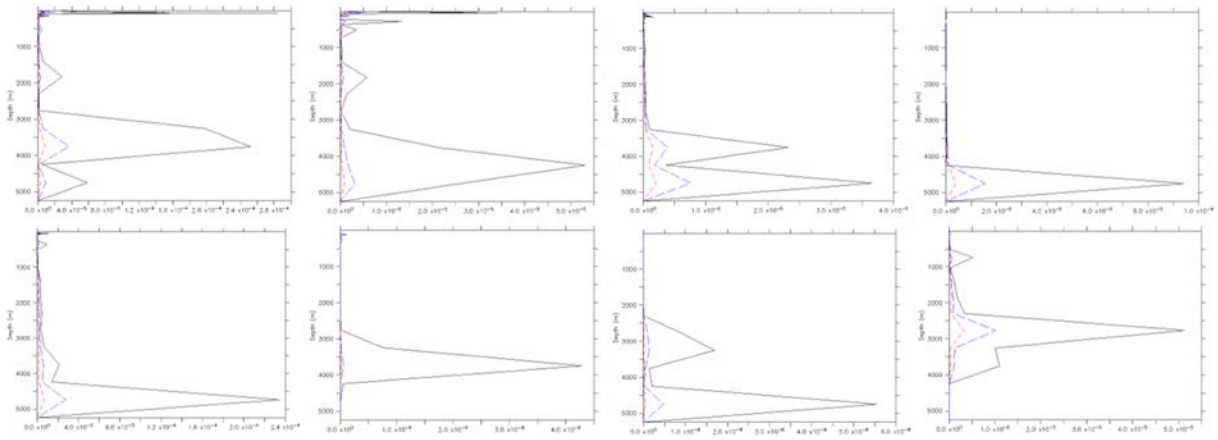

Figure 10. Vertical profile of negatively buoyant plastics (PVC, PS, PET, and PUR) (black line = control simulation, red dashed line = 90 m year^{-1} simulation, and blue dashed line = 30 m year^{-1} simulation)—(a) North Pacific, (b) South Pacific, (c) North Atlantic, (d) South Atlantic, (e) Indian, (f) Arctic, (g) Southern Oceans, and (h) Mediterranean Sea (NB = differing scales). Shown is the basin averaged plastic volumetric concentration normalized by the global average.

the lower sedimentation rate of 30 m year^{-1} and the control experiment, which is evident when comparing the plastic flux into the "sediments" at the sea floor (Figures 11a and 11b).

Plastic sedimentation tends to be large near shallow coastal areas. This is particularly evident along the east coast of South America, the west and south coast of Africa, within the coastal regions of Southeast Asia, and in the Indian Ocean (Figures 11a and 11b). This removal also occurs once the plastics reach the deep ocean, which can be seen in the Indian Ocean and in the Guinea Basin, as well as a number of other regions. The plastic flux in Southeast Asia and the Indian Ocean suggest that these are likely "hot spots" for plastic debris within the sediments. It has been suggested that there may be up to 4×10^9 microplastic fibers per square kilometer within the Indian Ocean, which would total approximately 1.4×10^9 metric tons in the Indian Ocean alone, based on an average fiber mass of 0.05 g (Coppock et al., 2017; Morét-Ferguson et al., 2010; Woodall et al., 2014). The Bohai Sea is the site of largest sedimentation fluxes in the ocean. Although there are very few empirical data for the Bohai Sea region, recent estimates of average microplastic abundances of 171.8 items per kg of dry weight sediment, comparable to abundances in harbor sediments in Belgium (Zhao et al., 2018).

The flux of plastics into the sediments in the Arctic Ocean is very pronounced in Figure 10f, with a reduction to near zero in both of the sensitivity experiments. This flux is focused in the Norwegian and Barents seas, as seen in Figures 11a and 11b. The relative paucity of plastics in the Arctic in these sensitivity experiments can

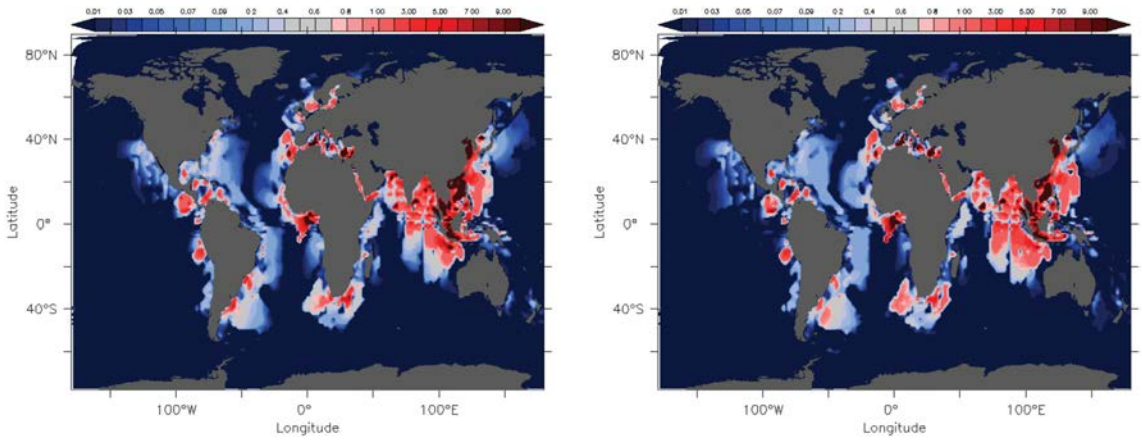

Figure 11. Flux of negatively buoyant plastics (PVC, PS, PET, and PUR) into the "sediments" at the end of a 50 year simulation, relative to the average global flux of plastics into the "sediments" per unit area with (a) 90 m year^{-1} piston velocity and (b) 30 m year^{-1} piston velocity.

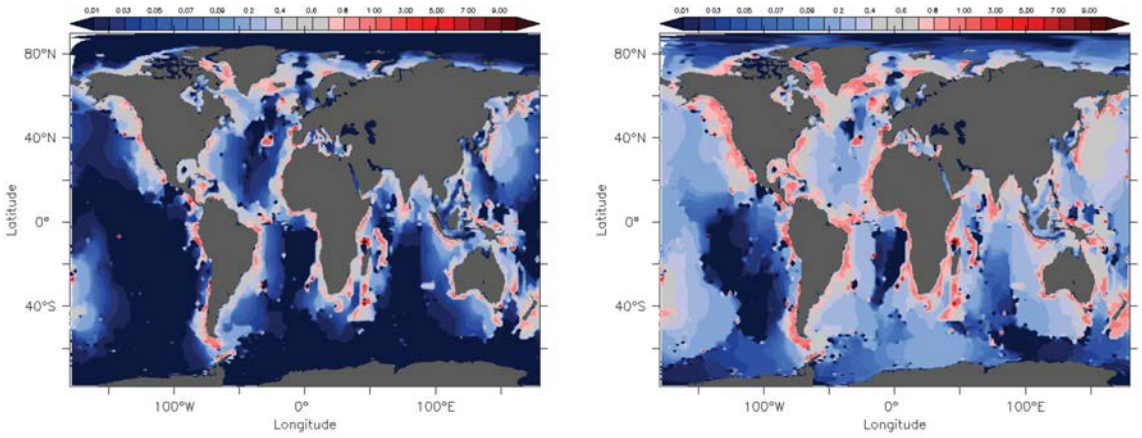

Figure 12. Difference between the concentration of negatively buoyant plastics (PVC, PS, PET, and PUR) in the control simulation and the sensitivity simulation with (a) 90 m year^{-1} piston velocity and (b) 30 m year^{-1} piston velocity after a 50 year simulation, relative the global average concentration of plastics.

also be observed in Figure 12a and 12b. Extensive sampling by Cózar et al. (2017) has confirmed high concentrations of plastic fragments in the northern and eastern areas of the Barents and Greenland Seas, with a scarcity or absence of plastic pollution in other areas. Further sampling within the Barents Sea (south of Svalbard) by Buhl-Mortensen and Buhl-Mortensen (2017), estimates that based on mean offshore litter density, a conservative quantification of the total plastic litter in the Barents Sea alone would amount to approximately 80 million metric tons. Considering the high plastic concentrations observed and global circulation patterns, the Arctic Ocean has been proposed as a potential "dead end" for plastic pollution (Cózar et al., 2017). If this is the case, it is to be expected that much of the plastic pollution imported into the Arctic would eventually be transported downward through the water column, suggesting that the Arctic sediments would also likely be a sink for plastic pollution. Continued observations at the HAUSGARTEN observatory, at about 2,500 m depth, in the eastern Fram Strait have shown that levels of litter at the seafloor in the Arctic have been increasing from 2002 to 2014 (Bergmann & Klages, 2012; Tekman et al., 2017), with mean litter densities of 6,566 items km^{-2} in the HAUSGARTEN area in 2014. These levels are comparable to litter densities in the Lisbon Canyon, in close proximity to Lisbon, a heavily populated city (Mordecai et al., 2011).

3.3. Neutrally Buoyant Sensitivity Simulation

A separate experimental simulation with neutrally buoyant plastics, that is with no rise velocity so that they behave as entirely passive tracers, was conducted. The results from this simulation show an almost ubiquitous distribution of neutrally buoyant plastics after 50 years of integration (Figure 13), with only some areas of the Southern and Arctic oceans with negligible plastic pollution. The Mediterranean Sea and Southeast Asia (particularly the Sea of Japan and Yellow Sea) show particularly high accumulations of these neutrally buoyant plastics, as well as the North Pacific and Indian Ocean to a lesser extent (Figure 13).

The neutrally buoyant plastics are present at all depths in the ocean, notably above 3,500 m, although there are substantially more of these plastics within the top 1,000 m in comparison to from 1,000 to 4,000 m (Figures 14a–14h). The North Atlantic, Arctic, Mediterranean, and Sea of Japan are the areas in which large quantities of neutrally buoyant plastics reach the deep water. These are all areas of deep water formation and with sizeable concentrations of plastics near the surface, which results in plastics drawn down into the deep ocean by vertical convection in the model. Plastics in surface waters from the North Atlantic may be transported into the Mediterranean, before sinking in the east, forming the Mediterranean Intermediate Water. Mediterranean Intermediate Water circulates westward, spilling over into the North Atlantic at depth and can be recognized at depths of around 1,000–1,200 m in the northern areas of the North Atlantic (Bryden & Stommel, 1984; Millot & Taupier-Letage, 2005). This is visible in Figure 13, as plastic components can be seen being flowing out of the Strait of Gibraltar.

The diffusion of positively, neutrally and negatively buoyant plastics is shown in Figures 15a–15c, as the global average concentration per depth (in tons km^{-3}) over the 50 year simulation period. The positively buoyant plastics are heavily concentrated within the top 100 m by the end of the 50 years, with visible seasonal

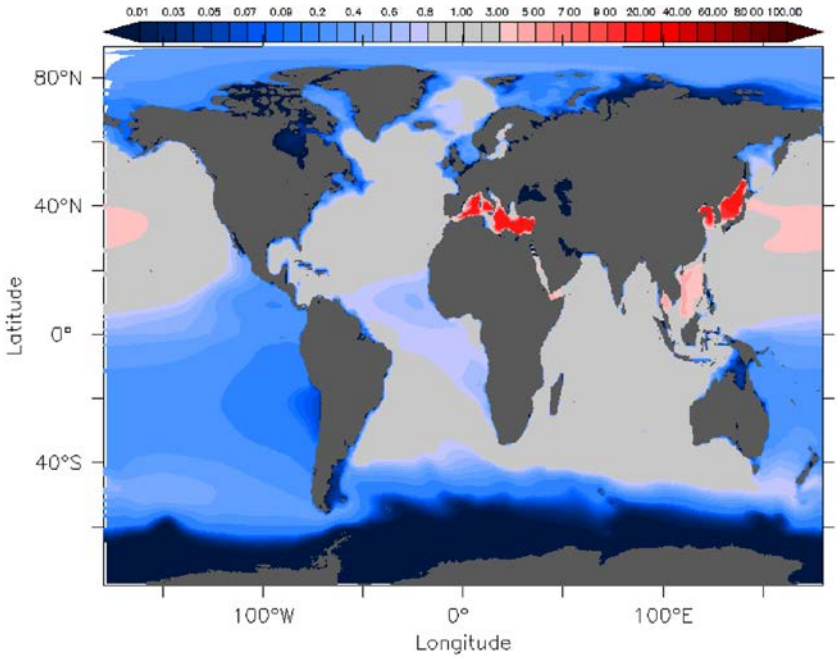

Figure 13. Accumulation of neutrally buoyant plastics after a 50 year simulation in the control experiment. Shown is the plastic concentration relative to the global average concentration of plastics.

cycles of downward mixing and upwellings drawing the plastics down to depths of between 200 and 300 m (Figure 15a). The neutrally buoyant plastics diffuse rapidly over 50 years down to the permanent thermocline at depths of nearly 1,500 m, with the highest concentrations within the top 200 m (Figure 15b). For the negatively buoyant plastics, there are a number of different depths of accumulation; at the near surface, where the plastics settle around the coastlines (as can be seen in Figure 9), a slight accumulation between 1,500 and 2,000 m on the continental slopes, and two higher concentration accumulations at 3,500–4,000 m and around 4,500 m, where the plastics settle on the deep ocean floor (Figure 15c), which can be correlated with the hypsometry of the ocean (Figure 15d). Given the extent to which these neutrally buoyant plastics have been shown to be transported, it may be appropriate to include a category of neutrally buoyant microplastics and nanoplastics in future modeling work, especially since, as we have argued, microplastics are essentially neutrally buoyant.

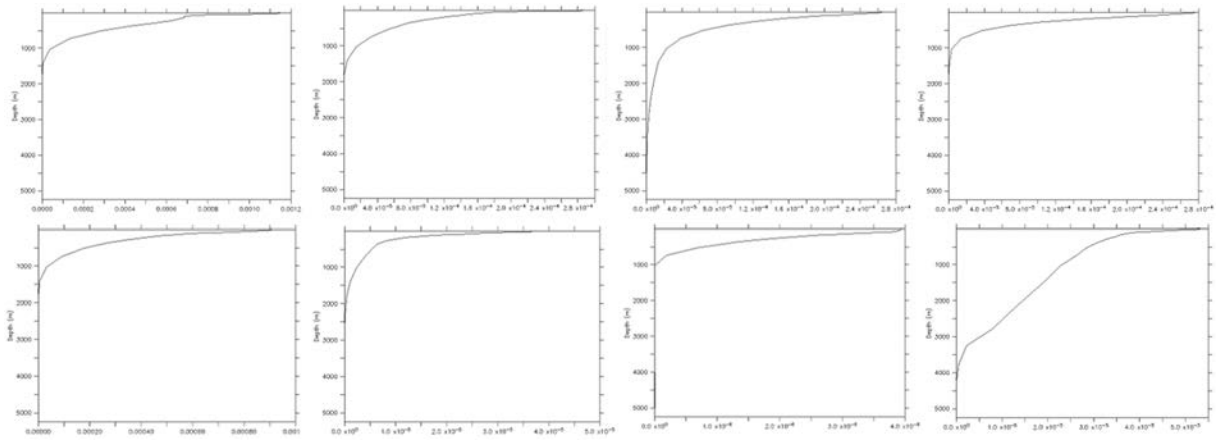

Figure 14. Vertical profile of neutrally buoyant plastics—(a) North Pacific, (b) South Pacific, (c) North Atlantic, (d) South Atlantic, (e) Indian Ocean, (f) Arctic, (g) Southern Ocean, and (h) Mediterranean Sea (NB = differing scales). Shown is the basin averaged plastic volumetric concentration normalized by the global average.

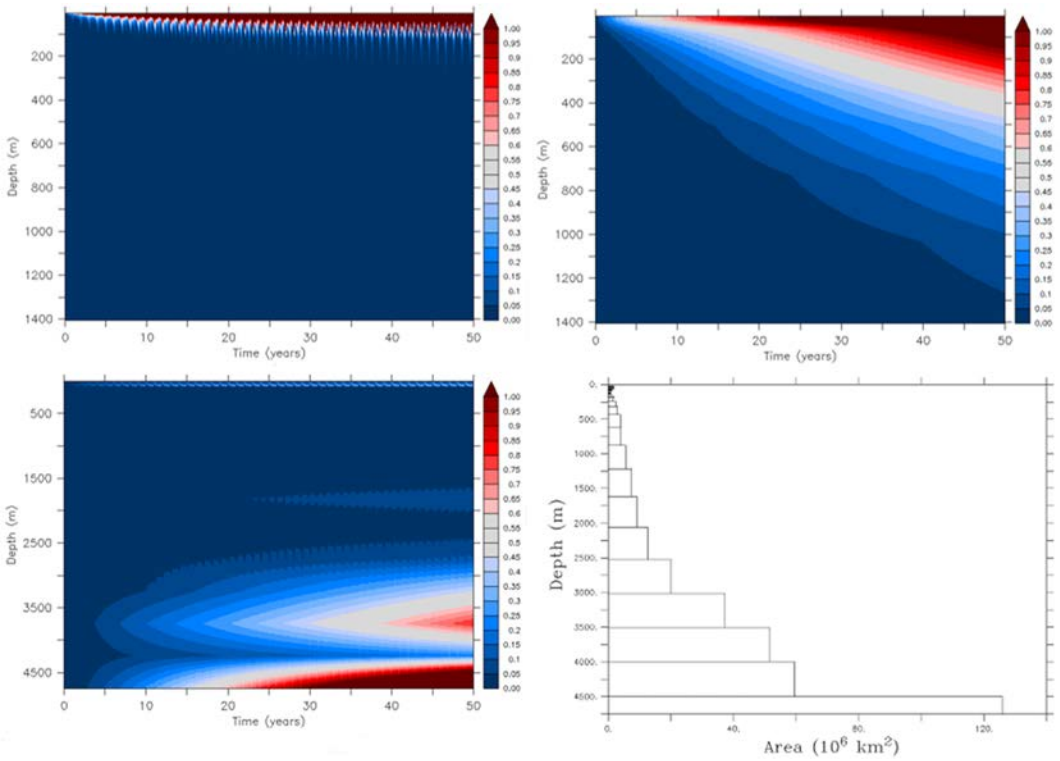

Figure 15. Average global concentration (tons km^{-3}) of (a) positively buoyant, (b) neutrally buoyant and (c) negatively buoyant plastics over a 50 year simulation, and (d) the global hypsometry of the ocean.

4. Conclusions

This is the first model to use an Eulerian formulation of plastic dispersion in the world's ocean, including a range of both positively and negatively buoyant plastic types. It is also the first to take into account the whole water column and apply a representation, admittedly crude, of the removal of plastics into the ocean sediments. With up to 70% of plastic debris entering the marine environment being negatively buoyant, it is important to include at least one negatively buoyant plastic component when modeling the distribution of marine plastic pollution. The inclusion of these negatively buoyant plastics reveals that there is likely widespread, high accumulation of plastics within coastal areas and in the deepest parts of the sea floor. While the sedimentation parameterisation developed in the simulations of this study was merely exploratory, it suggests that the sediments are likely to be a substantial sink for negatively buoyant plastic debris. Plastic particles have been found in sediments from the Arctic to the Mariana Trench, suggesting that plastics are most likely present ubiquitously within the ocean sediments. Sampling efforts need to be increased in order to more thoroughly map the distribution of plastics in sediments and also to provide accurate estimations of the levels the plastics reach to aid model verification.

There are a number of ways in which this model could be improved upon. Most pressingly, the improvement of plastic-sediments interaction and the inclusion of biological and physical-chemical processes that affect plastic once it enters the marine environment, such as biofouling and degradation over time. Laboratory or in situ research into these processes to provide accurate timescales and density changes for inclusion in model simulations would provide a more realistic representation. Eriksen et al. (2014) included a range of plastic particle sizes (from small microplastics to macroplastics) in their model, displaying the difference in modeled particle density and plastic mass distributions. However, once again these plastic particles only accounted for the floating portion of marine plastic debris. As discussed, microplastics and nanoplastics may in practice become neutrally buoyant, with the potential to disperse within the water column as virtually neutral passive tracers, completely at the will of ocean currents and turbulence. Therefore, the inclusion of a neutrally buoyant microsized to nanosized plastic component will be necessary in future modeling work.

Progress is being made toward standardization of methodologies in marine plastic sampling, separation and quantification, through a variety of projects and institutions. However, the difficulty in comparing the results from the present study to modeling research conducted in the past highlights the need for standardization within the field of marine plastic modeling as well as with plastic sampling methods.

Acknowledgments
Data are available on Zenodo at 10.5281/zenodo.3375589. We would like to thank Erik van Sebille for providing us with plastic input data. This research has been partly funded through the UKRI-NERC project CAMPUS (Combining Autonomous observations and Models for Predicting and Understanding Shelf seas) under Grant NE/R006776/1. We also acknowledge the support of SCOR (Scientific Committee on Oceanic Research) through the Working Group 153 on Floating Litter and its Oceanic TranSport Analysis and Modelling (FLOTSAM).

References

Alling, V., Sanchez-Garcia, L., Porcelli, D., Pugach, S., Vonk, J. E., Van Dongen, B., et al. (2010). Nonconservative behavior of dissolved organic carbon across the Laptev and East Siberian seas. *Global Biogeochemical Cycles*, *24*, GB4033. https://doi.org/10.1029/2010GB003834

Andrady, A. L., & Neal, M. A. (2009). Applications and societal benefits of plastics. *Philosophical Transactions of the Royal Society B: Biological Sciences*, *364*(1526), 1977–1984. https://doi.org/10.1098/rstb.2008.0304

Barnes, D. K. A. (2005). Remote islands reveal rapid rise of southern hemisphere sea debris. *The Scientific World Journal*, *5*, 915–921. https://doi.org/10.1100/tsw.2005.120

Barnes, D. K. A., Galgani, F., Thompson, R. C., & Barlaz, M. (2009). Accumulation and fragmentation of plastic debris in global environments. *Philosophical Transactions of the Royal Society B: Biological Sciences*, *364*(1526), 1985–1998. https://doi.org/10.1098/rstb.2008.0205

Batchelor, G. K. (1967). *An introduction to fluid dynamics*, (p. 615). Cambridge, U.K.: Cambridge University Press.

Beckmann, A., & Döscher, R. (1997). A method for improved representation of dense water spreading over topography in geopotential-coordinate models. *Journal of Physical Oceanography*, *27*(4), 581–591. https://doi.org/10.1175/1520-0485(1997)027<0581:AMFIRO>2.0.CO;2

Belamari, S., & Pirani, A. (2007). Validation of the optimal heat and momentum fluxes using the ORCA2-LIM global ocean-ice model. MERSEA Integrated Project, Tech. Rep., 88 pp.

Bergmann, M., & Klages, M. (2012). Increase of litter at the Arctic deep-sea observatory HAUSGARTEN. *Marine Pollution Bulletin*, *64*(12), 2734–2741. https://doi.org/10.1016/j.marpolbul.2012.09.018

Björk, G. (1989). A one-dimensional time-dependent model for the vertical stratification of the upper Arctic Ocean. *Journal of Physical Oceanography*, *19*(1), 52–67. https://doi.org/10.1175/1520-0485(1989)019<0052:AODTDM>2.0.CO;2

Blanke, B., & Delecluse, P. (1993). Variability of the tropical Atlantic ocean simulated by a general circulation model with two different mixed layer physics. *Journal of Physical Oceanography*, *23*(7), 1363–1388. https://doi.org/10.1175/1520-0485(1993)023<1363:VOTTAO>2.0.CO;2

Bowin, C. (1973). Origin of the Ninety East Ridge from studies near the equator. *Journal of Geophysical Research*, *78*(26), 6029–6043. https://doi.org/10.1029/JB078i026p06029

Bryden, H. L., & Stommel, H. M. (1984). Limiting processes that determine basic features of the circulation in the Mediterranean-Sea. *Oceanologica Acta*, *7*, 289–296.

Buhl-Mortensen, L., & Buhl-Mortensen, P. (2017). Marine litter in the Nordic Seas: Distribution composition and abundance. *Marine Pollution Bulletin*, *125*(1-2), 260–270. https://doi.org/10.1016/j.marpolbul.2017.08.048

Chiba, S., Saito, H., Fletcher, R., Yogi, T., Kayo, M., Miyagi, S., et al. (2018). Human footprint in the abyss: 30 year records of deep-sea plastic debris. *Marine Policy*, *96*, 204–212. https://doi.org/10.1016/j.marpol.2018.03.022

Coppock, R. L., Cole, M., Lindeque, P. K., Queirós, A. M., & Galloway, T. S. (2017). A small-scale, portable method for extracting microplastics from marine sediments. *Environmental Pollution*, *230*, 829–837. https://doi.org/10.1016/j.envpol.2017.07.017

Corcoran, P. L., Norris, T., Ceccanese, T., Walzak, M. J., Helm, P. A., & Marvin, C. H. (2015). Hidden plastics of Lake Ontario, Canada and their potential preservation in the sediment record. *Environmental Pollution*, *204*, 17–25. https://doi.org/10.1016/j.envpol.2015.04.009

Cózar, A., Echevarría, F., González-Gordillo, J. I., Irigoien, X., Úbeda, B., Hernández-León, S., et al. (2014). Plastic debris in the open ocean. *Proceedings of the National Academy of Sciences*, *111*(28), 10239–10244. https://doi.org/10.1073/pnas.1314705111

Cózar, A., Martí, E., Duarte, C. M., García-de-Lomas, J., van Sebille, E., Ballatore, T. J., et al. (2017). The Arctic Ocean as a dead end for floating plastics in the North Atlantic branch of the Thermohaline Circulation. *Science Advances*, *3*(4), e1600582. https://doi.org/10.1126/sciadv.1600582

Derraik, J. G. B. (2002). The pollution of the marine environment by plastic debris: A review. *Marine Pollution Bulletin*, *44*(9), 842–852. https://doi.org/10.1016/s0025-326x(02)00220-5

Dong, S., Gille, S. T., & Sprintall, J. (2007). An assessment of the Southern Ocean mixed layer heat budget. *Journal of Climate*, *20*(17), 4425–4442. https://doi.org/10.1175/JCLI4259.1

Eriksen, M., Lebreton, L. C. M., Carson, H. S., Thiel, M., Moore, C. J., Borerro, J. C., et al. (2014). Plastic pollution in the world's oceans: More than 5 trillion plastic pieces weighing over 250,000 tons afloat at sea. *PLoS ONE*, *9*(12), e111913. https://doi.org/10.1371/journal.pone.0111913

Frias, J., Gago, J., Otero, V., & Sobral, P. (2016). Microplastics in coastal sediments from Southern Portuguese shelf waters. *Marine Environmental Research*, *114*, 24–30. https://doi.org/10.1016/j.marenvres.2015.12.006

Gent, P. R. (2011). The Gent–McWilliams parameterization: 20/20 hindsight. *Ocean Modelling*, *39*(1-2), 2–9. https://doi.org/10.1016/j.ocemod.2010.08.002

Geyer, R., Jambeck, J. R., & Law, K. L. (2017). Production, use, and fate of all plastics ever made. *Science Advances*, *3*(7), e1700782. https://doi.org/10.1126/sciadv.1700782

Gilligan, M. R., Pitts, R. S., Richardson, J. P., & Kozel, T. R. (1992). Rates of accumulation of marine debris in Chatham County, Georgia. *Marine Pollution Bulletin*, *24*(9), 436–441. https://doi.org/10.1016/0025-326X(92)90342-4

Gregory, M. R. (2009). Environmental implications of plastic debris in marine settings—Entanglement, ingestion, smothering, hangers-on, hitch-hiking and alien invasions. *Philosophical Transactions of the Royal Society B: Biological Sciences*, *364*(1526), 2013–2025. https://doi.org/10.1098/rstb.2008.0265

Gyory, J., Bischof, B., Mariano, A. J., & Ryan, E.H. (2005). The Guinea current. Available at: http://oceancurrents.rsmas.miami.edu/atlantic/guinea.html (Accessed: 20/10/2017).

Hale, R. C. (2018). Are the risks from microplastics truly trivial? *Environmental Science & Technology*, *52*(3), 931–931. https://doi.org/10.1021/acs.est.7b06615

Hardesty, B. D., Harari, J., Isobe, A., Lebreton, L., Maximenko, N., Potemra, J. T., et al. (2017). Using numerical model simulations to improve the understanding of micro-plastic distribution and pathways in the marine environment. *Frontiers in Marine Science*, *4*, 30.
Hartmann, N., Hüffer, T., Thompson, R. C., Hassellöv, M., Verschoor, A., Daugaard, A. E., et al. (2019). Are we speaking the same language? Recommendations for a definition and categorization framework for plastic debris. *Environmental Science & Technology*, *53*(3), 1039–1047. https://doi.org/10.1021/acs.est.8b05297
IOC, SCOR and IAPSO (2010). The international thermodynamic equation of seawater – 2010: Calculation and use of thermodynamic properties. Intergovernmental Oceanographic Commission, Manuals and Guides No. 56, UNESCO (English), 196 pp.
Jambeck, J. R., Geyer, R., Wilcox, C., Siegler, T. R., Perryman, M., Andrady, A., et al. (2015). Plastic waste inputs from land into the ocean. *Science*, *347*(6223), 768–771. https://doi.org/10.1126/science.1260352
Kooi, M., Van Nes, E. H., Scheffer, M., & Koelmans, A. A. (2017). Ups and downs in the ocean: Effects of biofouling on the vertical transport of microplastics. *Environmental Science & Technology*, *51*(14), 7963–7971. https://doi.org/10.1021/acs.est.6b04702
Large, W. G., & Yeager, S. G. (2009). The global climatology of an interannually varying air-sea flux data set. *Climate Dynamics*, *33*(2-3), 341–364. https://doi.org/10.1007/s00382-008-0441-3
Law, K. L. (2017). Plastics in the marine environment. *Annual Review of Marine Science*, *9*, 205–229. https://doi.org/10.1146/annurev-marine-010816-060409
Lebreton, L., Slat, B., Ferrari, F., Sainte-Rose, B., Aitken, J., Marthouse, R., et al. (2018). Evidence that the Great Pacific Garbage Patch is rapidly accumulating plastic. *Scientific Reports*, *8*(1), 4666. https://doi.org/10.1038/s41598-018-22939-w
Lebreton, L. C. M., Van der Zwet, J., Damsteeg, J.-W., Slat, B., Andrady, A., & Reisser, J. (2017). River plastic emissions to the world's oceans. *Nature Communications*, *8*(1), 15611. https://doi.org/10.1038/ncomms15611
Lebreton, L.-M., Greer, S. D., & Borrero, J. C. (2012). Numerical modelling of floating debris in the world's oceans. *Marine Pollution Bulletin*, *64*(3), 653–661. https://doi.org/10.1016/j.marpolbul.2011.10.027
Leith, D. (1987). Drag on nonspherical objects. *Aerosol Science and Technology*, *6*(2), 153–161. https://doi.org/10.1080/02786828708959128
Li, W. C. (2018). In E. Y. Zeng (Ed.), Microplastic Contamination in Aquatic Environments*Chapter 5—The occurrence, fate, and effects of microplastics in the marine environment*, (pp. 133–173). Elsevier.
Liubartseva, S., Coppini, G., Lecci, R., & Clementi, E. (2018). Tracking plastics in the Mediterranean: 2D Lagrangian model. *Marine Pollution Bulletin*, *129*(1), 151–162. https://doi.org/10.1016/j.marpolbul.2018.02.019
Locarnini, R. A., Mishonov, A. V., Antonov, J. I., Boyer, T. P., Garcia, H. E., Baranova, O. K., et al. (2013). World Ocean Atlas 2013, Volume 1: Temperature, S. Levitus, Ed., A. Mishonov Technical Ed., NOAA Atlas NESDIS 73, 40 pp.
Lusher, A. L., Tirelli, V., O'Connor, I., & Officer, R. (2015). Microplastics in Arctic polar waters: the first reported values of particles in surface and sub-surface samples. *Scientific Reports*, *5*(1), 14947. https://doi.org/10.1038/srep14947
Madec, G., & the NEMO team (2008). NEMO ocean engine. Note du Pôle de modélisation, Institut Pierre-Simon Laplace (IPSL), France, No 27, ISSN No 1288-1619.
Maximenko, N., Hafner, J., & Niiler, P. (2012). Pathways of marine debris derived from trajectories of Lagrangian drifters. *Marine Pollution Bulletin*, *65*(1-3), 51–62. https://doi.org/10.1016/j.marpolbul.2011.04.016
McDermott, K. L. (2016). Plastic pollution and the global throwaway culture: Environmental injustices of single-use plastic. ENV 434 Environmental Justice. Book 7.
Millot, C., & Taupier-Letage, I. (2005). Circulation in the Mediterranean Sea. In A. Saliot (Ed.), *The Mediterranean Sea*, (pp. 29–66). Berlin Heidelberg, Berlin, Heidelberg: Springer.
Mordecai, G., Tyler, P. A., Masson, D. G., & Huvenne, V. A. I. (2011). Litter in submarine canyons off the west coast of Portugal. *Deep Sea Research Part II: Topical Studies in Oceanography*, *58*(23-24), 2489–2496. https://doi.org/10.1016/j.dsr2.2011.08.009
Morét-Ferguson, S., Law, K. L., Proskurowski, G., Murphy, E. K., Peacock, E. E., & Reddy, C. M. (2010). The size, mass, and composition of plastic debris in the western North Atlantic Ocean. *Marine Pollution Bulletin*, *60*(10), 1873–1878. https://doi.org/10.1016/j.marpolbul.2010.07.020
Obbard, R. W., Sadri, S., Wong, Y. Q., Khitun, A. A., Baker, I., & Thompson, R. C. (2014). Global warming releases microplastic legacy frozen in Arctic Sea ice. *Earth's Future*, *2*(6), 315–320. https://doi.org/10.1002/2014EF000240
Pacanowski, R. C., & Gnanadesikan, A. (1998). Transient response in a Z-level ocean model that resolves topography with partial cells. *Monthly Weather Review*, *126*(12), 3248–3270. https://doi.org/10.1175/1520-0493(1998)126<3248:TRIAZL>2.0.CO;2
Peeken, I., Primpke, S., Beyer, B., Gütermann, J., Katlein, C., Krumpen, T., et al. (2018). Arctic sea ice is an important temporal sink and means of transport for microplastic. *Nature Communications*, *9*(1), 1505. https://doi.org/10.1038/s41467-018-03825-5
PlasticsEurope, 2017. Plastics - the Facts 2017: An analysis of European plastics production, demand and waste data. Available at: https://www.plasticseurope.org/en/resources/publications/274-plastics-facts-2017.
Redi, M. H. (1982). Oceanic isopycnal mixing by coordinate rotation. *Journal of Physical Oceanography*, *12*(10), 1154–1158. https://doi.org/10.1175/1520-0485(1982)012<1154:OIMBCR>2.0.CO;2
Reisser, J., Slat, B., Noble, K., du Plessis, K., Epp, M., Proietti, M., et al. (2015). The vertical distribution of buoyant plastics at sea: an observational study in the North Atlantic Gyre. *Biogeosciences*, *12*(4), 1249–1256. https://doi.org/10.5194/bg-12-1249-2015
Ryan, P. G. (2015). A Brief History of Marine Litter Research. In M. Bergmann, L. Gutow, & M. Klages (Eds.), *Marine Anthropogenic Litter*, (pp. 1–25). Springer International Publishing, Cham.
Tekman, M. B., Krumpen, T., & Bergmann, M. (2017). Marine litter on deep Arctic seafloor continues to increase and spreads to the North at the HAUSGARTEN observatory. *Deep Sea Research Part I: Oceanographic Research Papers*, *120*, 88–99. https://doi.org/10.1016/j.dsr.2016.12.011
Thompson, R. O. (1984). Observations of the Leeuwin current off Western Australia. *Journal of physical oceanography*, *14*(3), 623–628. https://doi.org/10.1175/1520-0485(1984)014<0623:OOTLCO>2.0.CO;2
Timmermann, R., Goosse, H., Madec, G., Fichefet, T., Ethe, C., & Dulière, V. (2005). On the representation of high latitude processes in the ORCALIM global coupled sea ice–ocean model. *Ocean Modelling*, *8*(1-2), 175–201. https://doi.org/10.1016/j.ocemod.2003.12.009
Turner, S., Horton, A. A., Rose, N. L., & Hall, C. (2019). A temporal sediment record of microplastics in an urban lake, London, UK. *Journal of Paleolimnology*, *61*(4), 449–462. https://doi.org/10.1007/s10933-019-00071-7
Van Cauwenberghe, L., Devriese, L., Galgani, F., Robbens, J., & Janssen, C. R. (2015). Microplastics in sediments: A review of techniques, occurrence and effects. *Marine Environmental Research*, *111*, 5–17. https://doi.org/10.1016/j.marenvres.2015.06.007
Van Cauwenberghe, L., Vanreusel, A., Mees, J., & Janssen, C. R. (2013). Microplastic pollution in deep-sea sediments. *Environmental Pollution*, *182*, 495–499. https://doi.org/10.1016/j.envpol.2013.08.013
van Sebille, E., England, M. H., & Froyland, G. (2012). Origin, dynamics and evolution of ocean garbage patches from observed surface drifters. *Environmental Research Letters*, *7*(4), 044040. https://doi.org/10.1088/1748-9326/7/4/044040

Van Sebille, E., Griffies, S. M., Abernathey, R., Adams, T. P., Berloff, P., Biastoch, A., et al. (2018). Lagrangian ocean analysis: Fundamentals and practices. *Ocean Modelling*, *121*, 49–75. https://doi.org/10.1016/j.ocemod.2017.11.008

van Sebille, E., Wilcox, C., Lebreton, L., Maximenko, N., Hardesty, B. D., Van Franeker, J. A., et al. (2015). A global inventory of small floating plastic debris. *Environmental Research Letters*, *10*(12), 124006. https://doi.org/10.1088/1748-9326/10/12/124006

Vancoppenolle, M., Fichefet, T., Goosse, H., Bouillon, S., Madec, G., & Morales Maqueda, M. A. (2009). Simulating the mass balance and salinity of Arctic and Antarctic sea ice. 1. Model description and validation. *Ocean Modelling*, *27*(1-2), 33–53. https://doi.org/10.1016/j.ocemod.2008.10.005

Wessel, C., Swanson, K., Weatherall, T., & Cebrian, J. (2019). Accumulation and distribution of marine debris on barrier islands across the northern Gulf of Mexico. *Marine Pollution Bulletin*, *139*, 14–22. https://doi.org/10.1016/j.marpolbul.2018.12.023

Wilcox, C., Van Sebille, E., & Hardesty, B. D. (2015). Threat of plastic pollution to seabirds is global, pervasive, and increasing. *Proceedings of the National Academy of Sciences*, *112*(38), 11899–11904. https://doi.org/10.1073/pnas.1502108112

Woodall, L. C., Sanchez-Vidal, A., Canals, M., Paterson, G. L. J., Coppock, R., Sleight, V., et al. (2014). The deep sea is a major sink for microplastic debris. *Royal Society Open Science*, *1*(4), 140317. https://doi.org/10.1098/rsos.140317

Zhao, J., Ran, W., Teng, J., Liu, Y., Liu, H., Yin, X., et al. (2018). Microplastic pollution in sediments from the Bohai Sea and the Yellow Sea, China. *Science of The Total Environment*, *640*, 637–645.

Zweng, M. M., Reagan, J. R., Antonov, J. I., Locarnini, R. A., Mishonov, A. V., Boyer, T. P., et al. (2013). World Ocean Atlas 2013. Volume 2, Salinity. S. Levitus, Ed., A. Mishonov Technical Ed.; NOAA Atlas NESDIS 74, 39 pp.